Test synopsis of:

The Effects of Radiation Type on the Tolerance of High-Power 4H-SiC Diodes

Zhiyun Luo, Ayayi C. Ahyi, Tianbing Chen, Akil Sutton, and Becca Haugerud, John D. Cressler
David C. Sheridan, John R. Williams, Paul W. Marshall, and Robert A. Reed

Abstract— Proton irradiation is used to probe the physics of 4H-SiC SBDs and nMOS capacitors for the first time. Both 4H-SiC SBD diodes and SiC MOS structures show excellent radiation tolerance under high-energy, high-dose proton exposure. Unlike for SiC JBS diodes, which show a strong increase in series resistance under proton irradiation, these SiC SBDs show very little forward I-V degradation after exposure to 63 MeV protons up to a fluence of $5x10^{13} p/cm^{-2}$. An improvement in reverse current after irradiation is also observed, which could be due to a proton annealing effect. The small but observable increase in blocking voltage for these SiC SBDs is attributed to a negative surface charge increase, consistent with earlier gamma results. Characterization of 4H-SiC nMOS capacitors shows that Q_{eff} and D_{it} changed a little after $7x10^{12} p/cm^{-2}$ exposure, but relatively more after $5x10^{13} p/cm^{-2}$ exposure. The resultant Q_{eff} change under proton irradiation was used to investigate the radiation induced changes to the blocking voltage in the SBD diodes, and showed good agreement with experimental data.

I. Introduction

The physical and electronic properties of silicon carbide (SiC) make it an attractive semiconductor material for high-temperature, radiation resistant, and high-power-handling electronic devices [1], [2]. Previous studies on radiation effects in SiC devices show that SiC-based neutron and charge particle detectors [4], [5], [6], dosimeters [7], and spectrometers, have excellent potential for operating in extreme radiation environments [6], [7], [8], [9].

High-energy particle bombardment, such as by proton, neutron, electron and pion irradiation, can create vacancies, interstitials, and their associated defects. These radiation-induced defects often produce energy states in the bandgap and therefore can influence the electrical properties of materials and devices. Different irradiation-induced defects can be observed if the particle type, energy, fluences are changed, or if the exposure temperature and material processing differ [10], [11], [12]. We have previously studied the effects of high-dose gamma irradiation on 4H-SiC Schottky Barrier Diodes (SBD) and MOS capacitors [13], [14], and proton irradiation on 4H-SiC Junction Barrier Schottky (JBS) diodes [15]. There was little observed degradation for the SiC SBDs after gamma radiation, but interestingly, a significant degradation of R_S an improvement in reverse characteristics after proton irradiation of the JBS diodes, potentially compromising their usefulness in power switching systems operating in extreme environments. Given the closely related structure of SBD and JBS diodes (a JBS diode is composed of both *pn* and SBD diodes), this anomalous difference in their radiation response was particularly surprising, and has not to date been fully understood. In addition, the measured blocking voltages (BV) of the post proton-irradiated diodes consistently increased by about 200 V compared to the un-irradiated devices, a rare instance when radiation exposure actually improves device performance [15]. In this paper, we present new results of proton radiation effects on both 4H-SiC SBDs and MOS capacitors aimed at providing better understand these anomalous results and to help understand the unique physics of the $SiC - SiO_2$ interface.

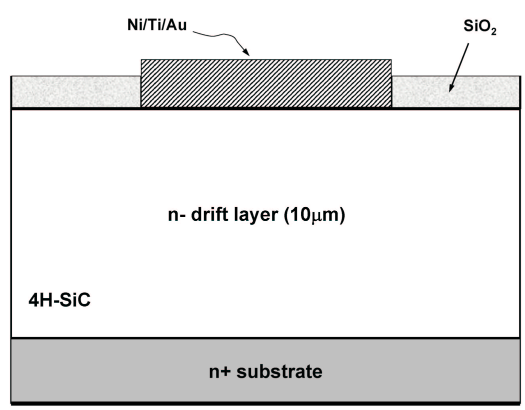

Fig. 1. A schematic device cross-section of the 4H-SiC SBD diode.

II. Experiment

Circular SBD diodes with diameters ranging from 100μm to 400μm were fabricated on 4H SiC n^+ wafers with a 10μm $1x10^{15} cm^{-3}$ n^- epitaxial layer obtained from Cree, Inc. A

This work was supported by NASA Cooperative Agreement No. NCC8-237, NASA Grant NAG3-2639, the Auburn University CSPAE, DTRA under the Radiation Tolerant Microelectronics Program, and NASA-GSFC under the Electronics Radiation Characterization Program, the AMSTC at Auburn University, and the Georgia Electronic Design Center at Georgia Tech.

Z. Luo is with the Alabama Microelectronics Science and Technology Center, Electrical and Computer Engineering Department, 200 Broun Hall, Auburn University, Auburn, AL 36849 USA (E-mail: lozhiyu@auburn.edu).

J.D. Cressler, T. Chen, A. Sutton, and B. Haugerud are with the School of Electrical and Computer Engineering, Georgia Institute of Technology, Atlanta, GA 30332, USA.

J.R. Williams and C. Ahyi are with the Physics Department, Auburn University, Auburn, AL 36849 USA.

D.C. Sheridan is with IBM Microelectronics, 1000 River Road, Essex Junction, VT, 05452 USA.

P.W. Marshall is a consultant to NASA-GSFC.

R.A. Reed is with NASA-GSFC, Code 562, Greenbelt , MD 20771, USA.

high quality thermal oxide followed by 1μm converted poly-Si layer was used for field passivation. Ni was deposited for the backside ohmic contacts and annealed at 1100 °C for 2 minutes in vacuum. Schottky contact openings were formed by selective RIE followed by a BOE etch through the passivation, and immediate loading into the metalization chamber for Ni schottky contact evaporation. Schottky contacts were completed with Ti and Au overlayers. This SBD metalization scheme was also used in the JBS diodes to facilitate unambiguous comparisons. A schematic cross-section of the device structure is shown in Figure 1.

4H-SiC nMOS capacitors were also fabricated to better understand the effects of radiation on the $SiC - SiO_2$ interface charge density. Prior to oxidation, the samples were cleaned using an RCA cleaning process followed by a dip in a buffered hydrogen fluoride solution. After the cleaning, the samples were immediately loaded into a double-walled oxidation furnace in an Ar atmosphere at room temperature. Dry oxidation was performed at 1150 °C for 2 hours to produce a 35 nm thick oxide layer. Samples were then loaded in Ar at 900 °C, and slowly raised to 1175 °C in Ar for the NO passivation step. The temperature was kept at 1175 °C for 2 hours in NO. Two layers of gate metals (100 nm of Mo plus 100 nm of Au) were deposited onto the oxide by conventional sputtering to form the MOS capacitors. For detailed fabrication of 4H-SiC MOS structures please refer to [14]. All MOS capacitors were circular, with diameters of 70, 200 and 340 μm.

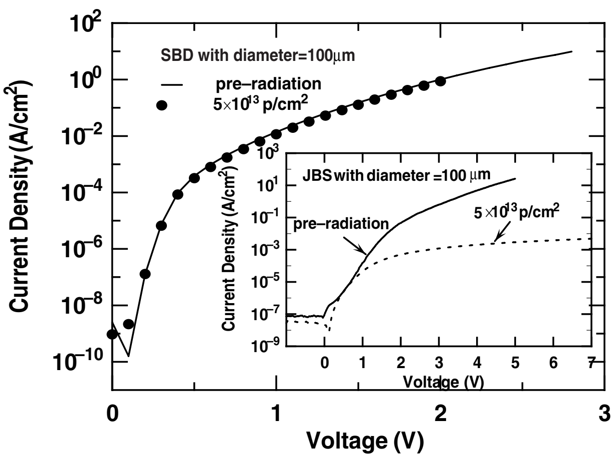

Fig. 2. Forward current-voltage characteristics of the 4H-SiC SBDs both before and after proton irradiation. Inset: forward current-voltage characteristics of 4H-SiC JBS diodes before and after proton irradiation

Proton irradiation was performed at the Crocker Nuclear Laboratory cyclotron located at the University of California at Davis, using 63.3 MeV protons. The SBDs and MOS capacitors were exposed to a fluences as high as $5x10^{13}p/cm^2$. Dosimetry measurements used a five-foil secondary emission monitor calibrated against a Faraday cup. The radiation source (Ta scattering foils) located several meters upstream of the target establish a beam spatial uniformity of about 15% over a 2.0 cm radius circular area. Beam currents from about 5 pA to 50 nA allow testing with proton fluxes from 1×10^6 to

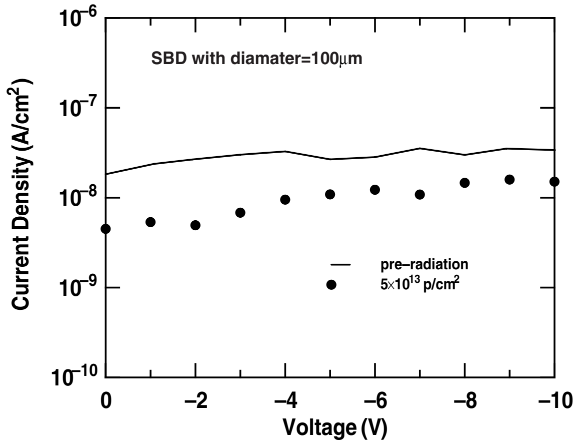

Fig. 3. Reverse current-voltage characteristics of the 4H-SiC SBDs both before and after proton irradiation.

1×10^{11} proton/cm^{2}sec. The dosimetry system is accurate to about 10%. At proton fluences of 1×10^{12} p/cm^2 and 5×10^{13} p/cm^2, the measured equivalent total ionizing dose was approximately 135 and 6,759 krad(Si), respectively. The SBDs and MOS capacitors were irradiated with all terminals floating, but previous results suggest that this does not have any impact on the results.

The forward and reverse current-voltage characteristics were measured with an Agilent 4155 Semiconductor Parameter Analyzer. Both forward and reverse characteristics were measured before and after irradiation. Reverse breakdown measurements were performed using a Tektronix 371 high-power curve tracer. The simultaneous Hi-Lo C-V (capacitance-voltage) method was used to measure effective oxide charge and the interface state density of the $SiC - SiO_2$ interface. High-frequency (Hi) C-V curves were measured at 100 kHz at room temperature to obtain the total effective oxide charge (Q_{eff}), which includes the oxide fixed charge, the oxide trapped charge, and any mobile ionic charge. Simultaneous Hi-Lo measurements were made at room temperature in order to extract the interface trap density (D_{it}).

III. Results and Discussion

A. SBD Diodes

All results in this section are based on measurements of 12 SBDs with 100μm diameter geometry, distributed across two different dies. The results are quite uniform among all of the diodes. Figure 2 shows a typical forward-bias characteristics of a SBD with oxide passivation, both before and after proton irradiation. The magnitude of the forward current density is repeatably slightly decreased for the irradiated sample, and can be attributed to the introduction of radiation induced trap levels in the forbidden gap by the incident protons. Such trap levels can readily capture free majority carriers, leading to a lower net current conduction [15], [16], [17]. As can be seen, the low injection portion of the J-V curve changes very little after radiation, and the ideality factor remains about 1.02 while the barrier height remains around 1.05 V, suggesting that proton radiation didn't degrade the schottky contact of the device. This is consistent with our previous results on JBS diodes. Note, however, that the high injection portion of the J-V characteristics show only negligible changes at $5x10^{13}p/cm^2$ fluence, which is profoundly different from that observed with proton irradiated JBS diodes (inset of Figure 2), where the series resistance (R_S) increased dramatically following proton exposure [15]. Considering the differences in the structures of the SBD and JBS diodes, this suggests that the R_S change observed in the JBS diodes is probably due to the radiation-induced degradation of the interface between metal and the p-type 4H-SiC. One other possibility is the p-type 4H-SiC material itself (found in pn junction portion of the JBS device) responds differently to protons than does the n-type 4H-SiC region (found in the SBD regions of the JBS diode), but this is unlikely.

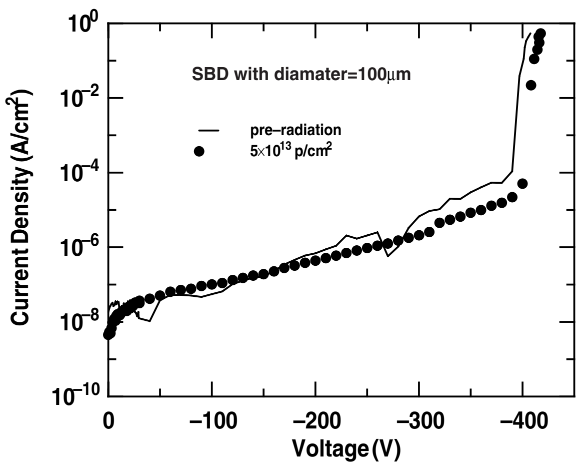

Fig. 4. Measured reverse leakage and blocking characteristics both before and after proton irradiation.

A small but repeatable decrease in the low voltage reverse-bias leakage current after proton exposure was also observed (Figure 3). The reverse current density of these SiC diodes decreases from $3.54x10^{-8}A/cm^2$ to $1x10^{-8}A/cm^2$ at 10 V of reverse bias. This result is similar to what was observed in the proton-irradiated JBS diodes. Figure 4 shows the measured reverse leakage and breakdown before and after proton irradiation. The reverse leakage after irradiation remains smaller than its pre-radiation values, although the pre-irradiation reverse current shows two clear and repeatable "kinks" at around 50 V and 270 V for these diodes. Interestingly, these kinks disappeared after proton exposure, suggesting that proton exposure has an annealing effect on certain deep level traps in 4H-SiC. Similar types of annealing effects using electron irradiation on SiC has been previously reported by [18], and similar radiation-induced reverse leakage improvements have also been observed [10].

As we can see from Figure 4, the blocking voltages for this SBD increase from 389 V to 413 V after proton exposure. The average increase for all the diodes is only 23 V, but statistically repeatable, and is much smaller than that observed for the JBS diodes. This is reasonable considering high series resistance of JBS diodes after proton irradiation. The relatively small blocking voltage increase of SBDs in the present work can also be attributed to the radiation-induced excess charge in the surface passivation layers [13]. To better understand these results, we determined the change in the oxide charge by analyzing the effects of proton irradiation on 4H-SiC MOS capacitors.

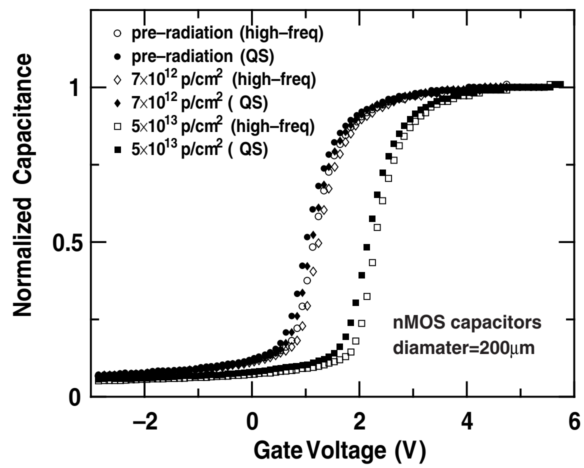

Fig. 5. Influence of proton irradiation on the C-V characteristics of the 4H-SiC MOS capacitors.

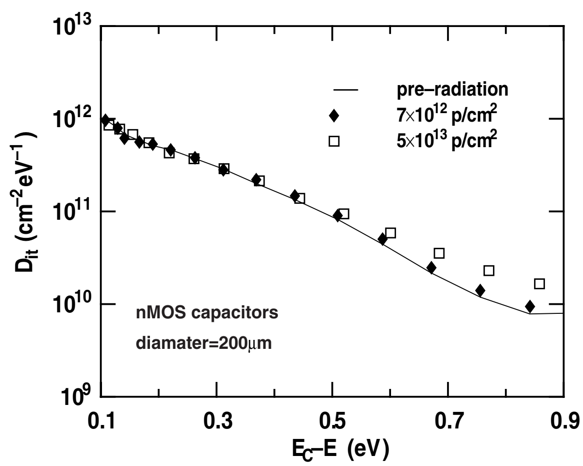

Fig. 6. Extracted interface state density of the 4H-SiC MOS capacitors both before and after proton irradiation.

B. MOS Capacitors

The radiation results reported here on nMOS capacitors are based on fourteen 200 μm diameter structures distributed on 2 different dies and are again quite uniform among these devices. Typical normalized CV curves from the nMOS capacitors before and after irradiation are shown in Figure 5. The results show that the 4H-SiC nMOS capacitors are radiation tolerant up to $7x10^{12}p/cm^2$ fluence. There is a very small positive shift in the CV curves after $7x10^{12}p/cm^2$ but a much large positive shift after $5x10^{13}p/cm^2$. The V_{FB} after the $5x10^{13}p/cm^2$ exposure shifts from 1.22 V to 2.34 V, and shows that the total proton exposure resulted in a net negative charge increase, consistent with our earlier results using gamma rays.

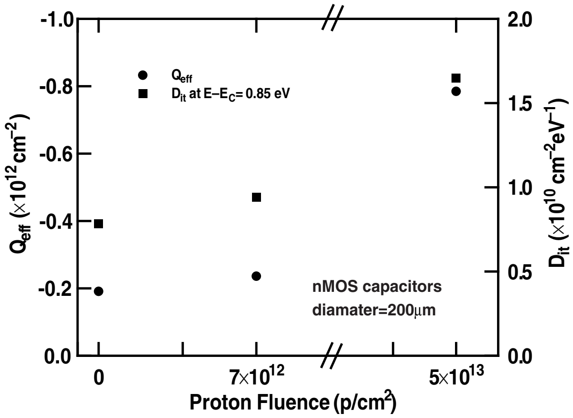

Fig. 7. Effective charge density and interface state density as functions of proton fluence.

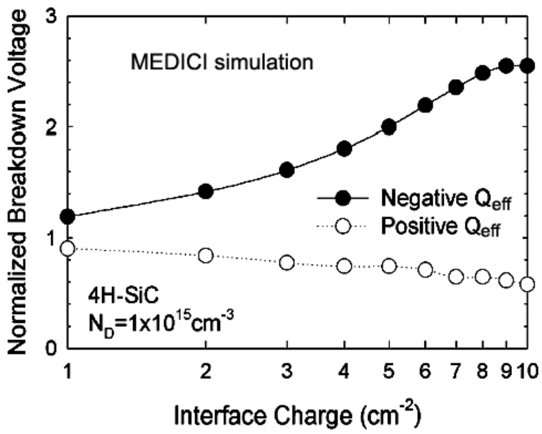

Fig. 8. Breakdown voltage change as a function of the radiation-induced interface charge density.

Figure 6 shows the extracted interface state density (D_{it}) as a function of energy level before and after irradiation. At energy levels close the conduction band edge, D_{it} remains unchanged even after $5x10^{13}p/cm^2$ fluence. As the energy level moves more deeply into the bandgap, however, the effects of radiation on D_{it} become distinct. Beyond $E_C - E$=0.85 eV, D_{it} become roughly constant for both the un-irradiated and irradiated samples. The Q_{eff} and D_{it} at $E_C - E$=0.85 eV as a function of proton fluence is shown in Figure 7. As can be seen, both Q_{eff} and D_{it} change only slightly after $7x10^{12}p/cm^2$ proton exposure, but more significantly after a fluence of $5x10^{13}p/cm^2$. Q_{eff} decreases (becomes more negative) by about $-7.1x10^{11}cm^{-2}$ at $5x10^{13}p/cm^2$, while D_{it} increases by $9x10^9cm^{-2}eV^{-1}$.

The measured changes in Q_{eff} were used to simulate the anticipated blocking voltage change in the SBD using MEDICI simulations [20]. Figure 8 shows the simulated effects on blocking voltage of radiation-induced negative and positive Q_{eff} as a function of interface charge density [13]. The measured change of $-7.1x10^{11}cm^{-2}$ in effective interface charge leads to an increase of about 20 V in blocking voltage [13] [14], consistent with our SBD device measurements. Thus, we believe that the measured SBD blocking voltage increase is primarily the result of the negative increase in oxide charge. With the increased negative surface charge, the potential contours under reverse bias are significantly spread out, thereby reducing the electric field crowding which leads to breakdown. This increase, however, is relatively small compared to that for SBDs irradiated with gamma rays [13], consistent with the differences in induced surface charge for both radiation types.

IV. Summary

4H-SiC SBDs and nMOS capacitors show a high level of radiation tolerance after proton exposure. Unlike for SiC JBS diodes, SiC SBDs show very little forward I-V degradation after exposure to proton fluences as high as $5x10^{13}p/cm^2$, suggesting that the proton-induced high R_S of the SiC JBS diodes after proton exposure is probably related to radiation-induced damage of contact metal and interface between metal and p-type SiC. The reverse leakage current of post-irradiated SiC SBDs shows decrease (improvement) after proton exposure, which could be due to proton annealing effects. The observed slight increase in blocking voltage for SiC SBDs after proton exposure is attributed to to an increase in negative surface charge.

Acknowledgment

The authors would like to thank T.F. Isaacs-Smith, S. Wang, C. Ellis, J. Jaeger, K. LaBel, L. Cohn, C. Marshall, C. Palor, and H. Kim for their contributions to this work.

References

[1] M. Bhatnagar and B.J. Baliga, IEEE Trans. Electron Devices, vol. 40, pp. 645-655, 1993.
[2] B.J. Baliga, Power Semiconductor Devices, Boston, MA: PWS, 1996.
[3] A.R. Dullo *et al*., IEEE Trans. Nuclear Science., vol. 46, pp. 275-279, 1999.
[4] F.H. Ruddy *et al*., IEEE Trans. Nuclear Science vol. 45, pp. 536-541, 1998.
[5] F. Nava *et al*., Material Science Forum vol. 353-C356, pp. 757-762, 2001.
[6] M. Rogalla *et al*., Nuclear Physics B Proc. Suppl., vol. 78, pp. 516-520, 1999.
[7] M. Bruzzi *et al*., Diamond and Related Materials, vol. 10, pp. 657-662, 2001.
[8] G. Bertuccio *et al*., em IEEE Trans. Nuclear Science vol. 48, pp. 232-233, 2001.
[9] S. Seshadri *et al*., IEEE Trans. Electron Devices, vol. 46, pp. 567-571, 1999.
[10] F. Navaa *et al*., Nuclear Instruments and Methods in Phys. Res. A, vol. 505, pp. 645C655, 2003.
[11] A.M. Strel'chuk *et al*., Materials Science and Engr. B, vol. 61-62, pp. 441-445, 1999.
[12] S. Nigam *et al*., Applied Physics Letters, vol. 81, pp. 2385-2387, 2002.
[13] D.C. Sheridan *et al*., IEEE Trans. Nuclear Science, vol. 48, pp. 2229-2232, 2000.
[14] T. Chen *et al*., Solid-State Electronics, vol. 46, pp. 2213-2235, 2002.
[15] Z. Luo *et al*., 2003 IEEE NSREC, Monterey, CA, paper A-8, July 2003.
[16] G.C. Messenger, IEEE Trans. Nuclear Science, vol. 39, pp. 468-473, 1992.
[17] J. McGarrity *et al*., IEEE Trans. Nuclear Science, vol. 39, pp. 1974-1981, 1992.
[18] W.A. Doolittle *et al*., Proc. Materials Research Society, Power Semi. Mater. and Devices Symp., Fall 1997, Boston, MA, pp. 197-202.
[19] H. Nielsena *et al*., Physica B, vol. 340-342, pp. 743-747, 2003.
[20] "MEDICI 2-D semiconductor device simulator," Avant! Corp., Palo Alto, CA, ver. 4.3, 1999.